

Supplementary material for LHCb-PAPER-2020-040

This appendix contains supplementary material that will be posted on the public CDS record but will not appear in the paper. Figure 1 shows the fit to $B^+ \rightarrow J/\psi K^+$ decays used to determine nuisance asymmetries. Figure 2 is the invariant mass of all candidates after the trigger and stripping, before additional cuts and BDT selection. Figures 3-4 are critical variables to the event selection, used in the trigger, BDT, or both. The signal component corresponds to simulated $B^+ \rightarrow K^+\pi^0$ decays, background is data from the mass sidebands ($m(K^+\pi^0) < 4860 \text{ MeV}/c^2$, $m(K^+\pi^0) > 5700 \text{ MeV}/c^2$). Figure 11 shows the raw $B^+ \rightarrow K^+\pi^0$ asymmetry between years and magnet polarities. Figure 12 shows the topology of the $B^+ \rightarrow K^+\pi^0$ decay.

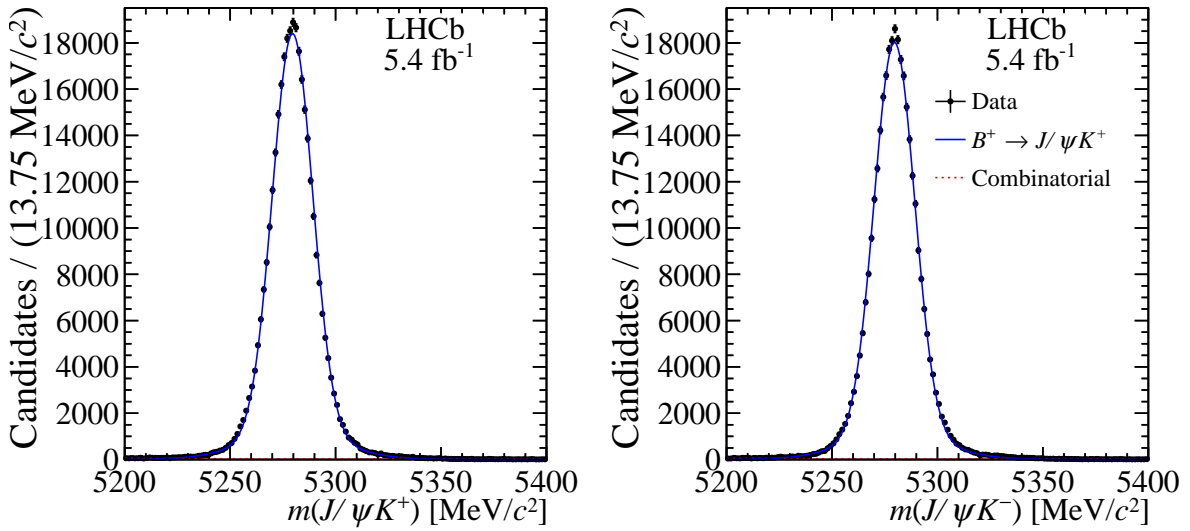


Figure 1: Invariant mass distribution of $B^+ \rightarrow J/\psi K^+$ candidates used to correct for nuisance asymmetries. The data is divided by the charge of the B meson, with $B^+ \rightarrow J/\psi K^+$ shown on the left and $B^- \rightarrow J/\psi K^-$ on the right.

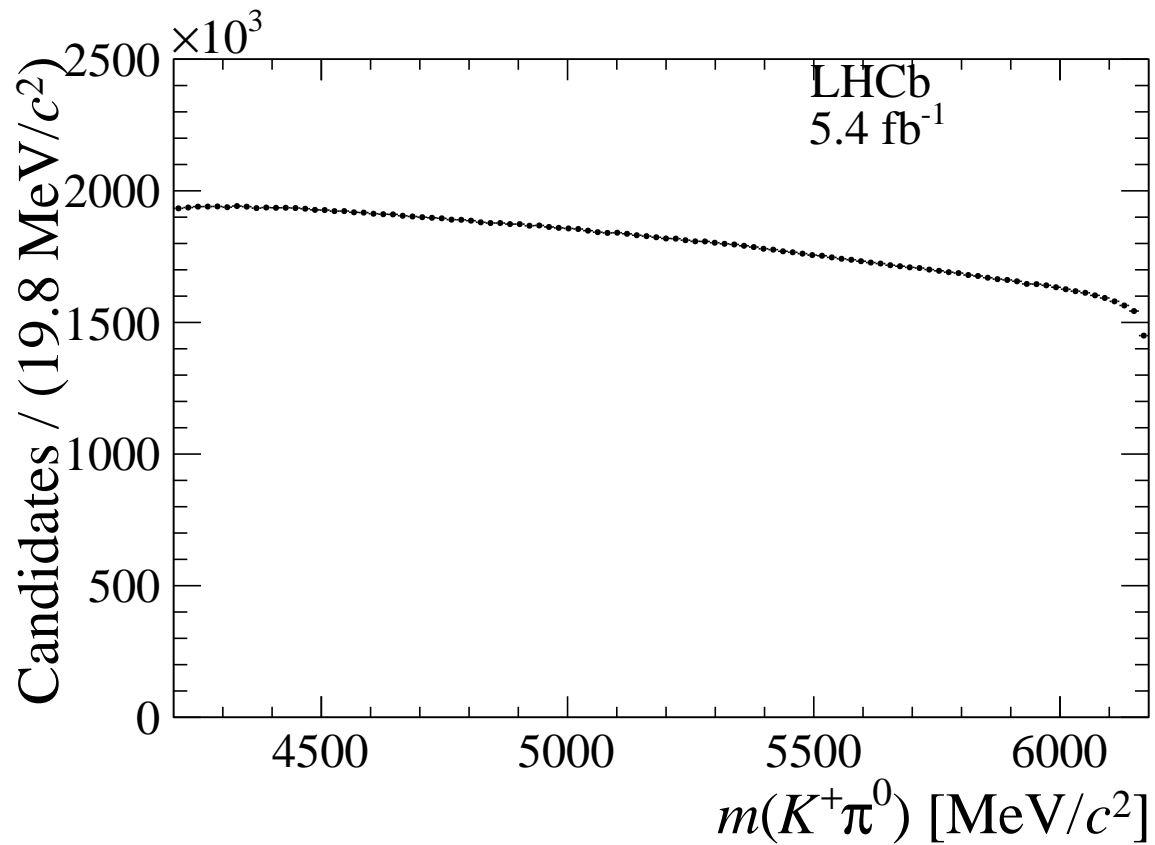


Figure 2: Invariant mass distribution of $B^+ \rightarrow K^+ \pi^0$ candidates after the initial candidate selection. The roll-off at high mass is due to differences in the online and offline reconstruction, particularly of neutral pions.

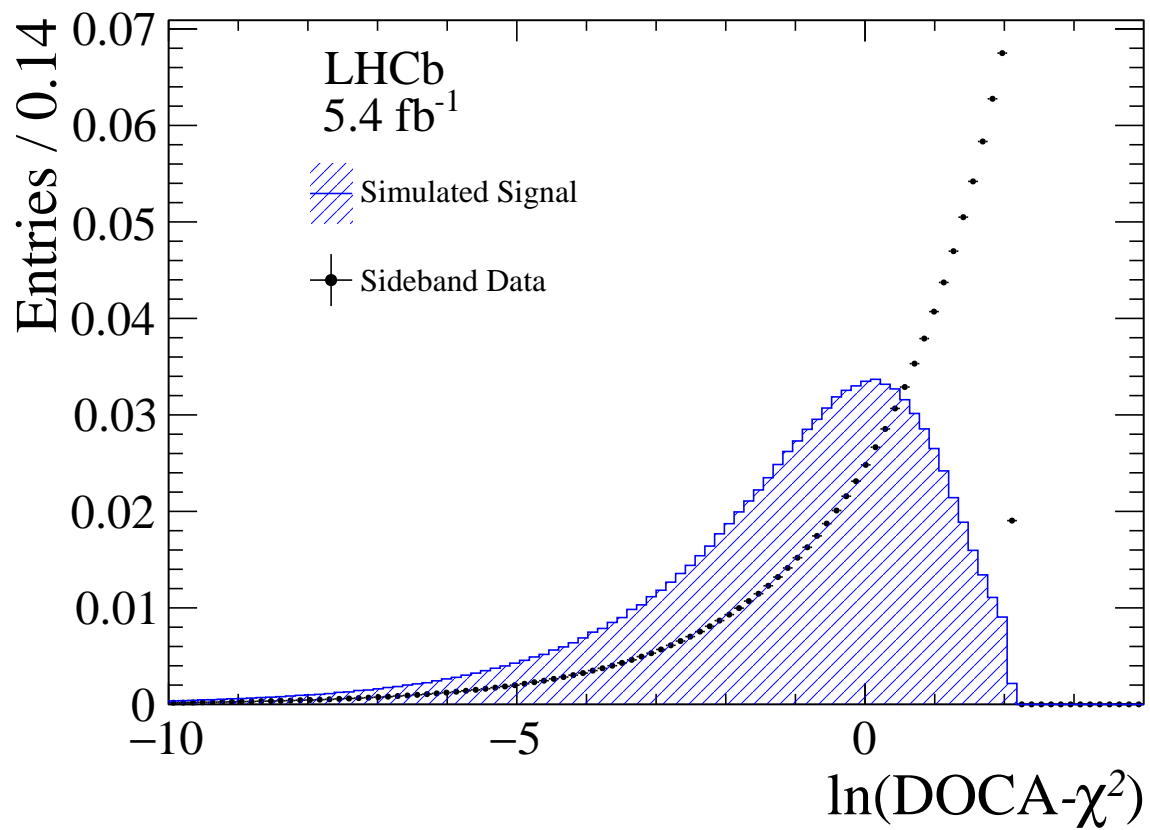


Figure 3: Signal and background distributions of DOCA- χ^2 after the initial candidate selection, normalized to unit area.

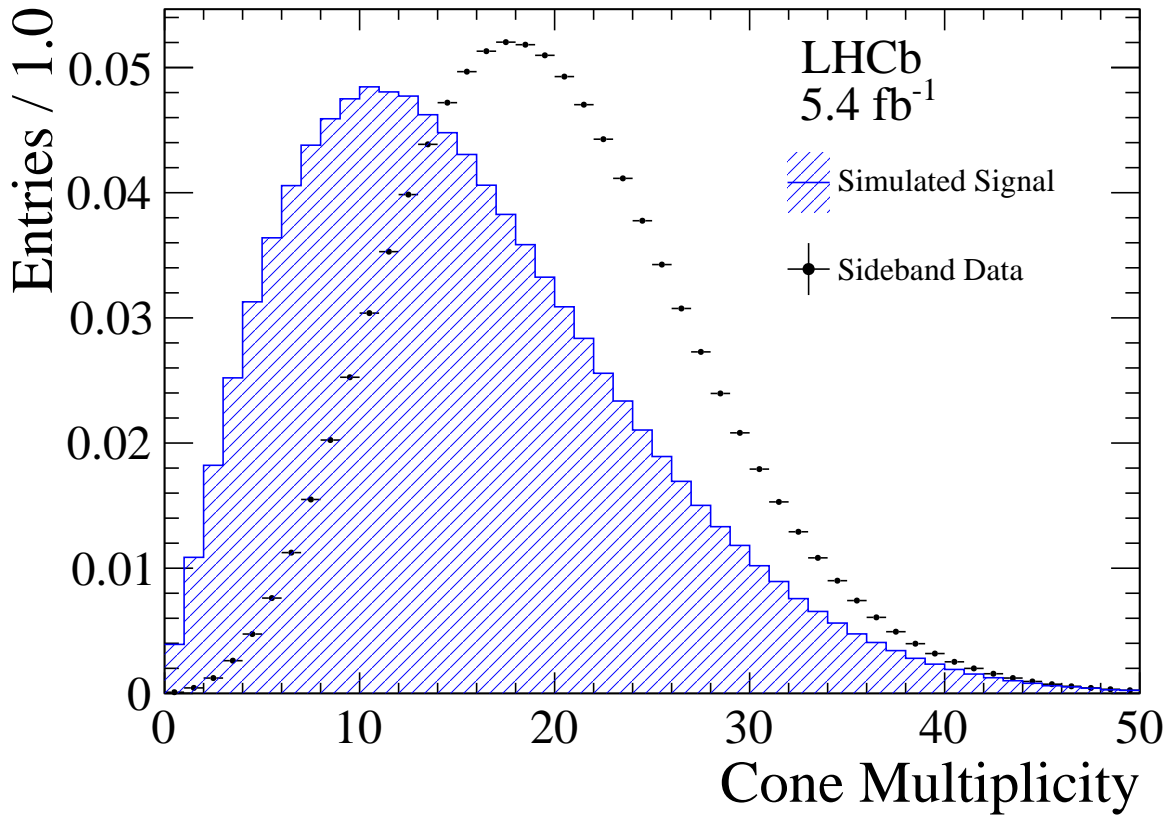


Figure 4: Signal and background distributions of multiplicity of tracks in a cone of $\Delta R = 1.7$ around the B^+ candidate trajectory after initial event selection, normalized to unit area.

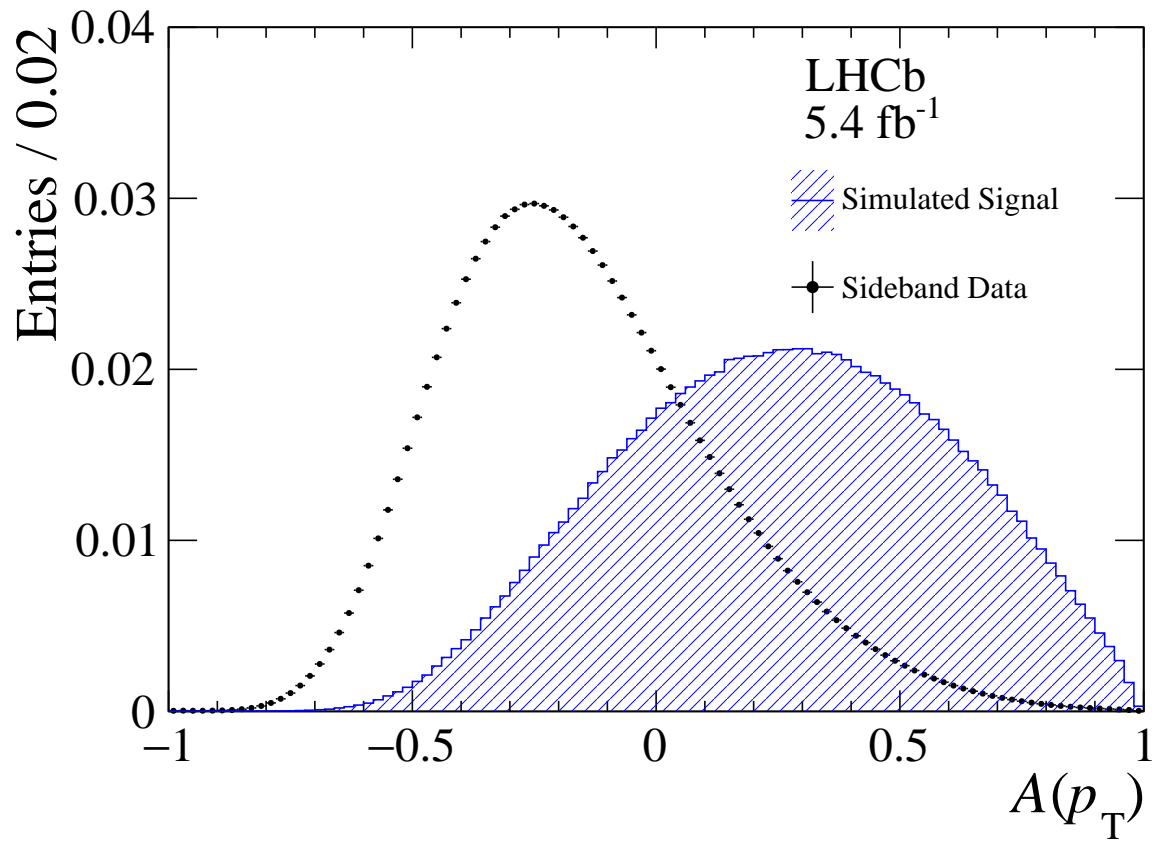


Figure 5: Signal and background distributions of p_T asymmetry in a cone of $\Delta R = 1.7$ around the B^+ candidate trajectory after the initial candidate selection, normalized to unit area.

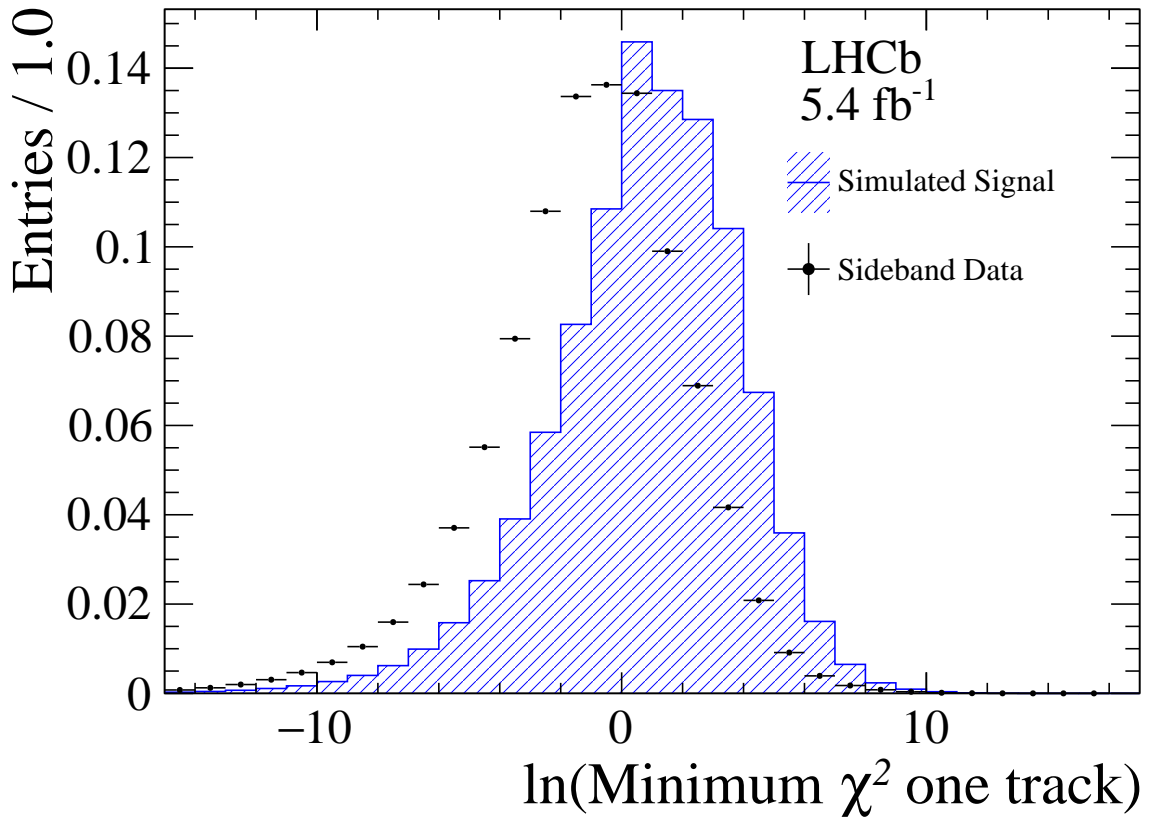


Figure 6: Signal and background distributions of the smallest χ^2 of vertex formed by adding one additional track to the K^+ after the initial candidate selection, normalized to unit area.

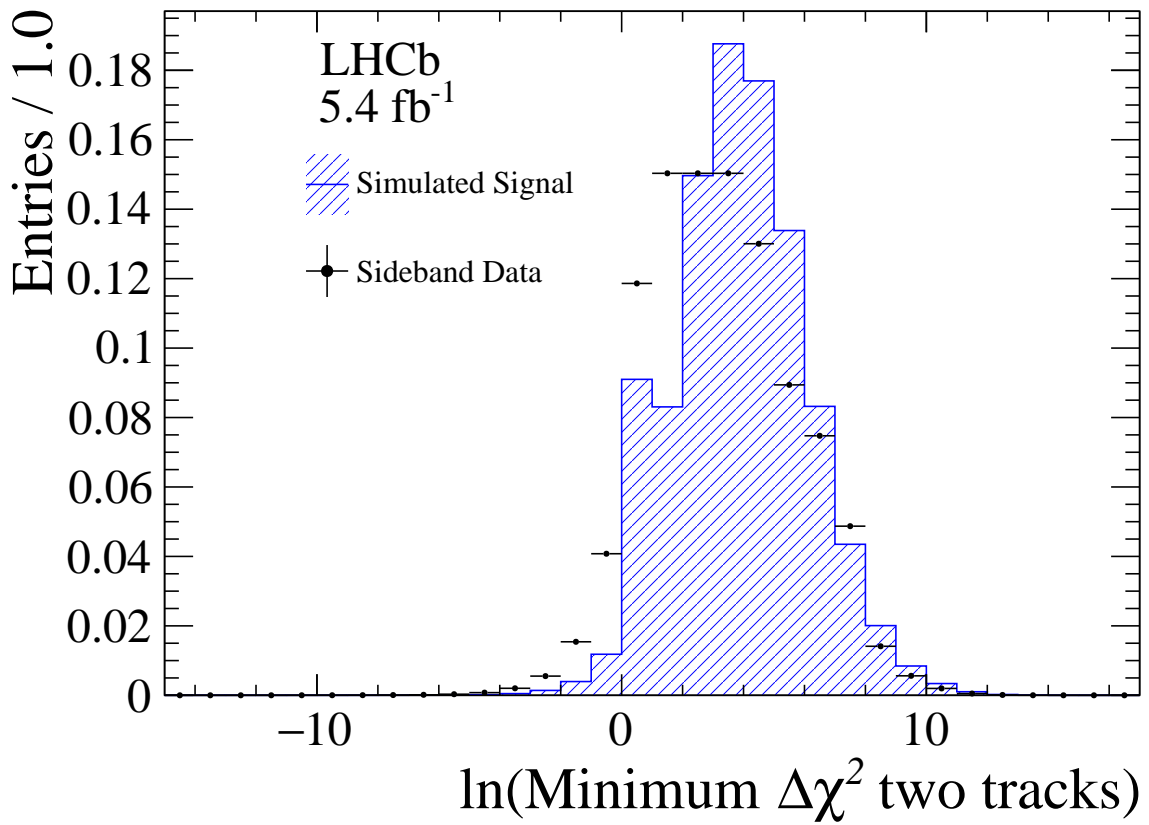


Figure 7: Signal and background distributions of the smallest $\Delta\chi^2$ of vertex formed by adding a second track to the lowest χ^2 vertex formed by adding one additional track to the K^+ after the initial candidate selection, normalized to unit area.

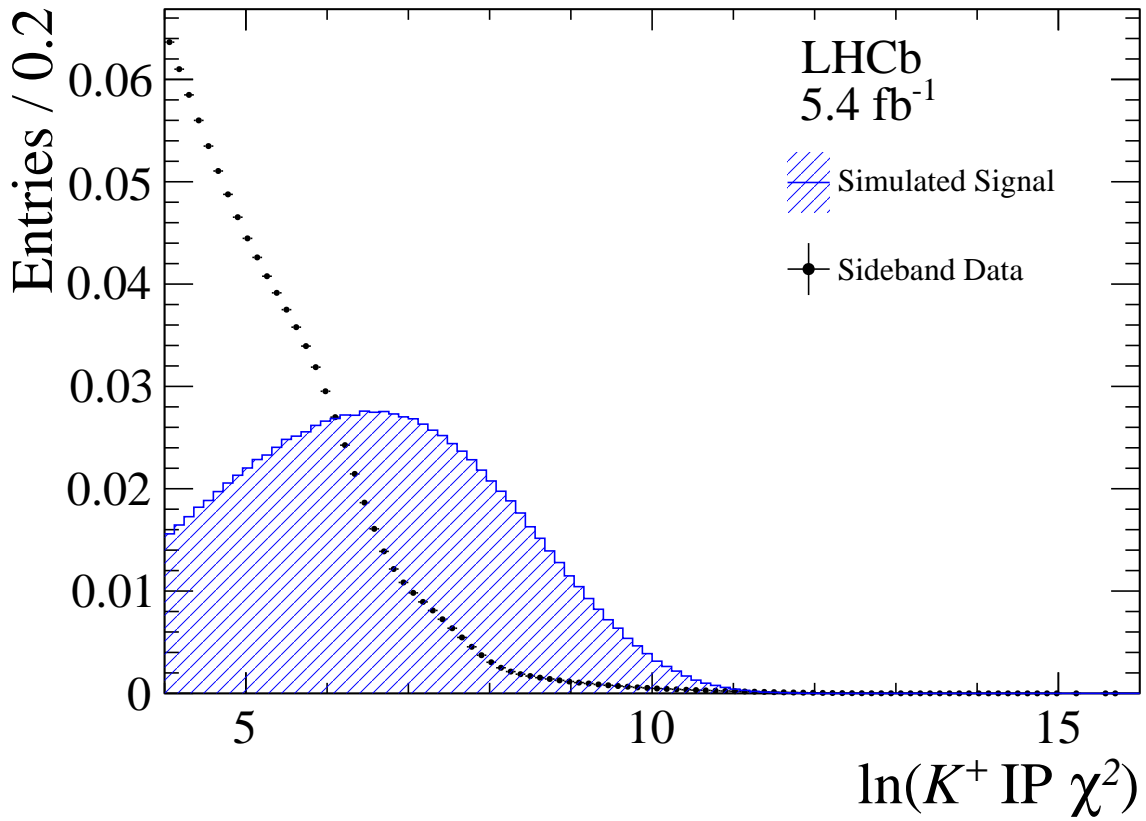


Figure 8: Signal and background distributions of the smallest change in χ^2 of the PV when including the K^+ in the vertex fit after the initial candidate selection, normalized to unit area.

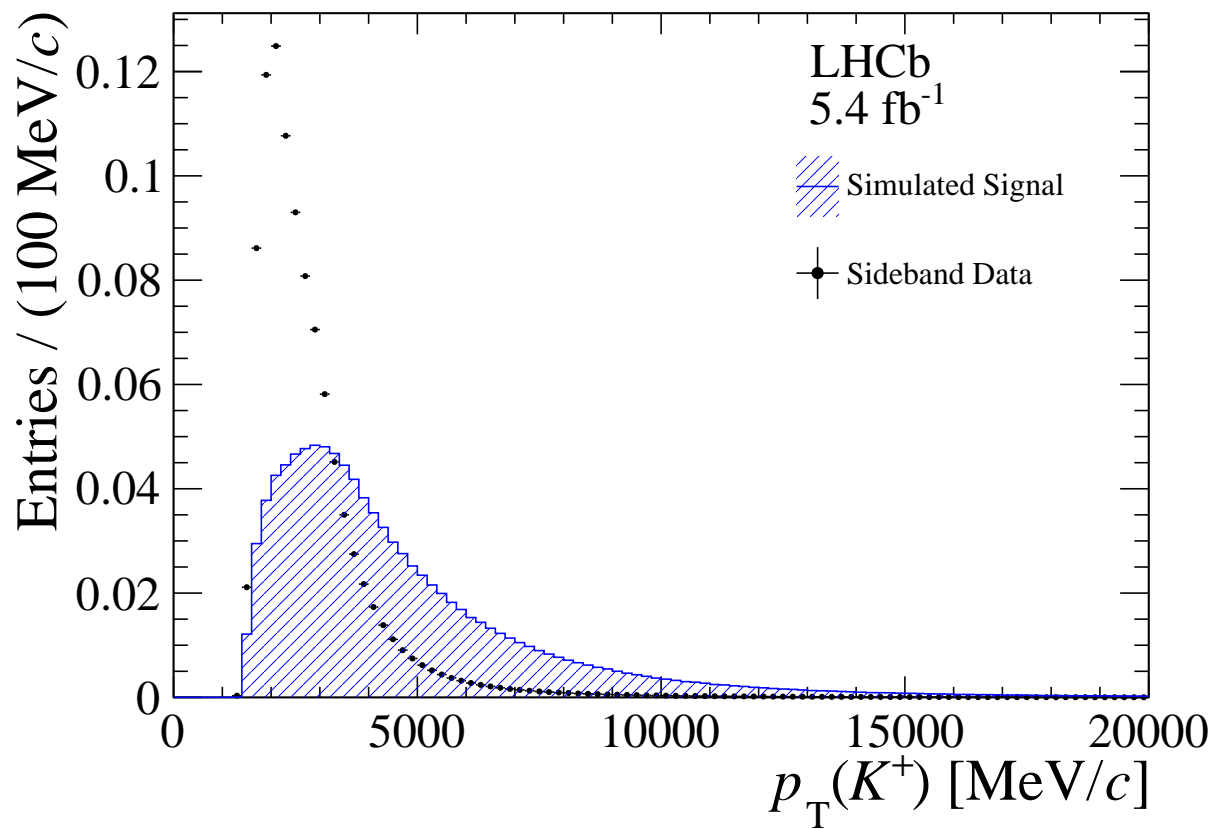


Figure 9: Signal and background distributions of K^+ p_T after the initial candidate selection, normalized to unit area.

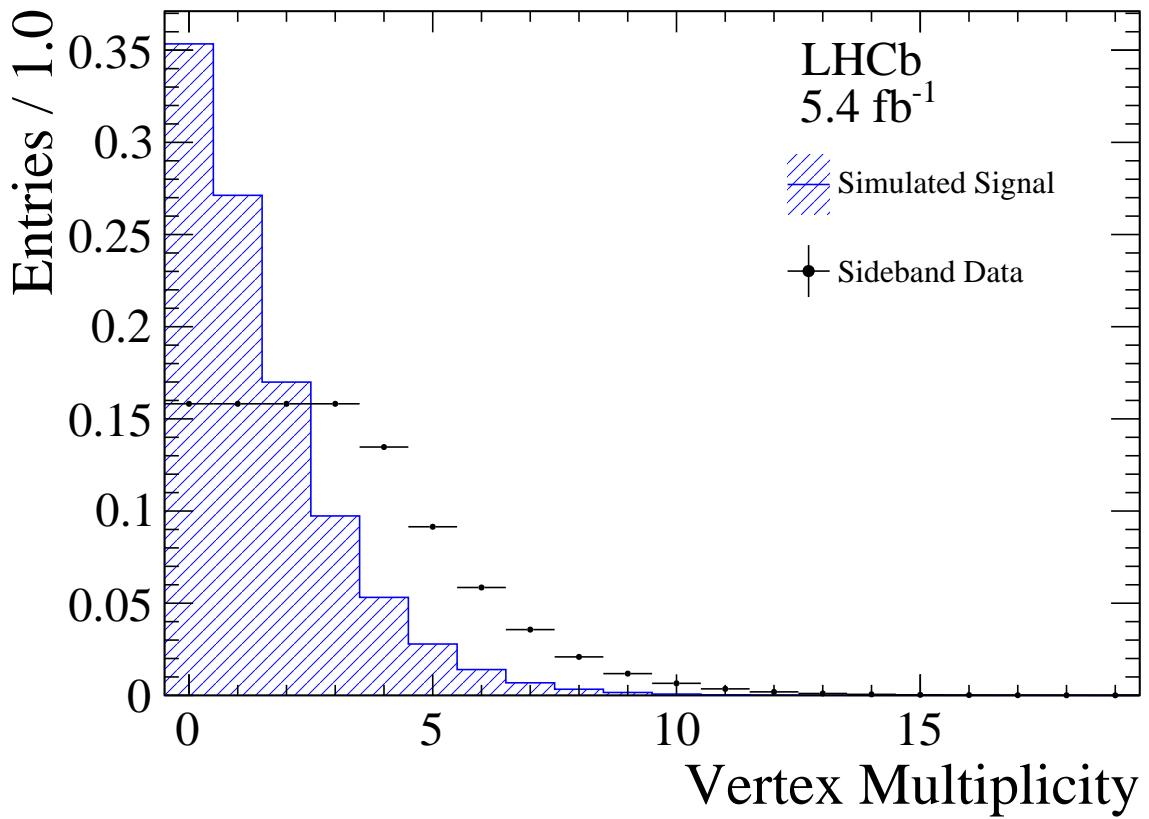


Figure 10: Signal and background distributions of multiplicity of vertices having small χ^2 after the initial candidate selection, normalized to unit area.

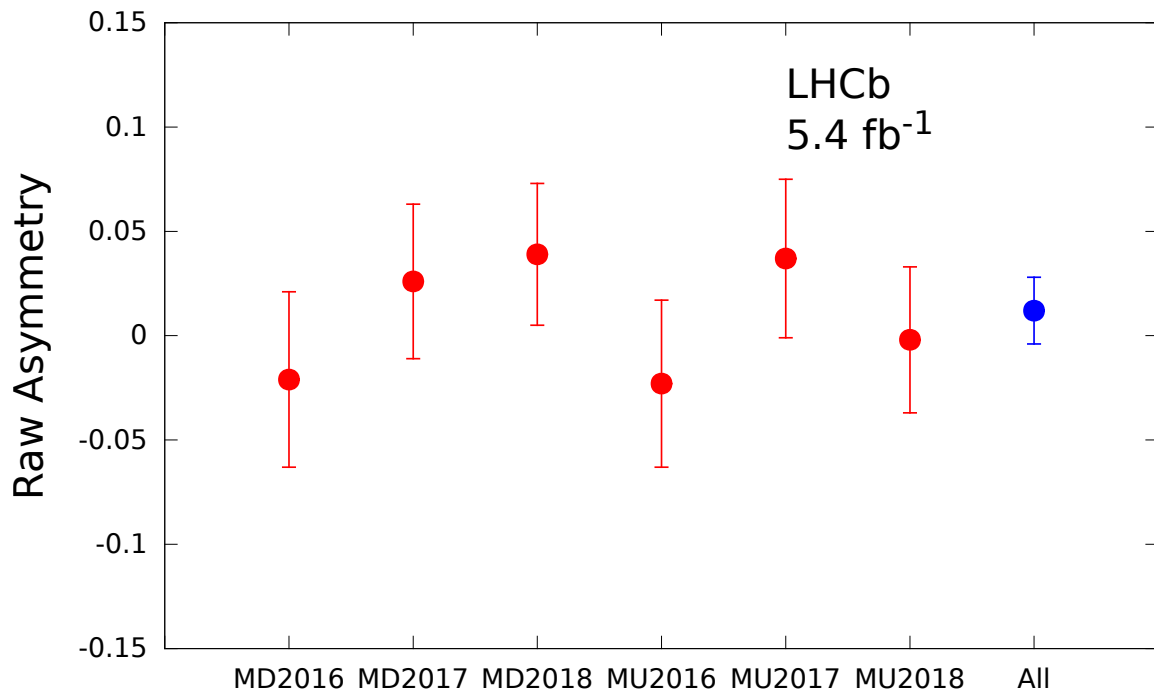


Figure 11: Raw asymmetries for $B^+ \rightarrow K^+ \pi^0$ separated by year and whether the magnetic field is aligned vertically upwards (MU) or downwards (MD)

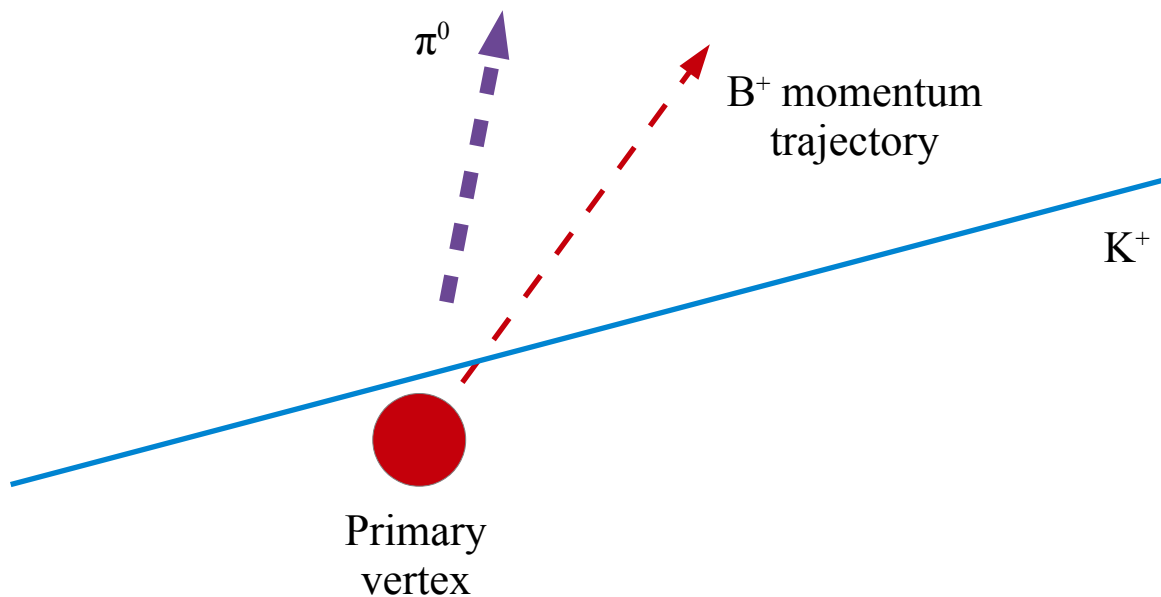


Figure 12: Diagram of the $B^+ \rightarrow K^+ \pi^0$ decay topology. The solid blue line represents the K^+ track, and the wide dashed purple line represents the reconstructed π^0 momentum. They are combined to form the B^+ momentum trajectory shown as a narrow red dashed line, which is assumed to originate from the primary vertex also shown in red.